Quaternary Research 83 (2015) 41–51

Contents lists available at ScienceDirect

Quaternary Research

journal homepage: www.elsevier.com/locate/yqres

Quantifying the contribution of sediment compaction to late Holocene salt-marsh sea-level reconstructions, North Carolina, USA

Matthew J. Brain [a,*], Andrew C. Kemp [b], Benjamin P. Horton [c,d], Stephen J. Culver [e], Andrew C. Parnell [f], Niamh Cahill [f]

[a] Department of Geography and Institute of Hazard Risk and Resilience, Durham University, South Road, Durham DH1 3LE, UK
[b] Department of Earth and Ocean Sciences, Tufts University, Medford, MA 02155, USA
[c] Institute of Coastal and Marine Science, Rutgers University, New Brunswick, NJ 08901, USA
[d] Division of Earth Sciences and Earth Observatory of Singapore, Nanyang Technological University, 639798, Singapore
[e] Department of Geological Sciences, East Carolina University, Greenville, NC 27858, USA
[f] School of Mathematical Sciences (Statistics), University College Dublin, Belfield, Dublin 4, Ireland

ARTICLE INFO

Article history:
Received 27 September 2013
Available online 12 September 2014

Keywords:
Post-depositional lowering
Tump Point
Salt-marsh peat

ABSTRACT

Salt-marsh sediments provide accurate and precise reconstructions of late Holocene relative sea-level changes. However, compaction of salt-marsh stratigraphies can cause post-depositional lowering (PDL) of the samples used to reconstruct sea level, creating an estimation of former sea level that is too low and a rate of rise that is too great. We estimated the contribution of compaction to late Holocene sea-level trends reconstructed at Tump Point, North Carolina, USA. We used a geotechnical model that was empirically calibrated by performing tests on surface sediments from modern depositional environments analogous to those encountered in the sediment core. The model generated depth-specific estimates of PDL, allowing samples to be returned to their depositional altitudes. After removing an estimate of land-level change, error-in-variables changepoint analysis of the decompacted and original sea-level reconstructions identified three trends. Compaction did not generate artificial sea-level trends and cannot be invoked as a causal mechanism for the features in the Tump Point record. The maximum relative contribution of compaction to reconstructed sea-level change was 12%. The decompacted sea-level record shows 1.71 mm yr^{-1} of rise since AD 1845.

Introduction

Late Holocene relative sea level (RSL) reconstructions supplement and extend spatially and temporally limited tide-gauge records to provide a context for current and projected rates of rise, and to capture multiple phases of sea-level behaviour for calibration of predictive models (Gehrels et al., 2011; Kemp et al., 2011; Bittermann et al., 2013). Sequences of salt-marsh sediment are a valuable archive for reconstructing RSL because salt marshes accrete sediment to preserve their elevation in the tidal frame under regimes of rising RSL where sediment supply is not limited, or where salt-marsh accretion primarily results from organogenic growth (Morris et al., 2002). However, samples of salt-marsh sediment used to reconstruct sea level may have undergone post-depositional lowering (PDL) by compaction of underlying sediment (Jelgersma, 1961; Bloom, 1964; Allen, 1999, 2000; van Asselen et al., 2009). PDL causes an over-estimation of the amount and rate of reconstructed sea-level rise (Horton and Shennan, 2009; Horton et al., 2013). The contribution of compaction must be quantified and removed from sea-level reconstructions to permit fair comparison among records and to ensure that the sensitivity of sea level to forcing factors is not misinterpreted or overstated.

Use of basal salt-marsh samples that directly overlie an incompressible substrate avoids the influence of compaction (Jelgersma, 1961; Donnelly et al., 2004), but compilations of discrete basal RSL reconstructions typically lack the chronological and vertical precision required to identify sub-millennial trends (see Engelhart and Horton, 2012). Therefore, late Holocene RSL reconstructions rely on samples from a single core of salt-marsh sediment (e.g., van de Plassche et al., 1998). One of the most detailed reconstructions of late Holocene RSL is from North Carolina (USA) (Kemp et al., 2009, 2011). It was developed using vertically-ordered samples of salt-marsh peat from two cores—one at Sand Point and one at Tump Point. After adjustment for land-level change, the record shows a sea-level rise in the first millennium and that the modern rate of sea-level rise is the greatest century-scale rise of the past two millennia (Kemp et al., 2011). However, the effect of compaction on these records was only qualitatively assessed and PDL may have contributed to the timing, magnitude and form of reconstructed sea-level trends (cf. Gehrels and Woodworth, 2013). If the key characteristics of the sea-level record are wholly or partially artefacts of sediment compaction, existing conclusions regarding climatic controls on global sea level may be erroneous (cf. Grinsted et al.,

* Corresponding author.
E-mail address: matthew.brain@durham.ac.uk (M.J. Brain).

http://dx.doi.org/10.1016/j.yqres.2014.08.003
0033-5894/

2011). Consequently, compaction-induced distortions of the sea-level record may have influenced the calibration of semi-empirical models relating sea level to global temperature (Kemp et al., 2011).

Sea-level reconstructions from cores of salt-marsh sediment can be corrected for the effects of compaction using geotechnical modelling (Pizzuto and Schwendt, 1997; Paul and Barras, 1998; see van Asselen et al., 2009, for a detailed summary of previous work). Brain et al. (2011, 2012) developed an empirical framework to estimate the magnitude and effects of compaction in a column of salt-marsh sediment. This model requires calibration by performing geotechnical tests on surface sediments from modern depositional environments analogous to those encountered in sedimentary archives. The model has not previously been applied to, or validated in, a real-world sedimentary succession (cf. Brain et al., 2012). Therefore, the accuracy of the model and ease with which the modern analogue approach can be applied to a particular core are unknown.

Our primary aim is to estimate the degree to which reconstructed sea-level trends in North Carolina result from sediment compaction by applying the Brain et al. (2011, 2012) geotechnical model to the Tump Point core of Kemp et al. (2009, 2011). We detail our calibration approach, outline our assumptions regarding the availability and suitability of modern analogues, and describe a model validation exercise that suggests our assumptions are reasonable. We quantify the contribution of compaction to late Holocene sea-level trends reconstructed in North Carolina and estimate that compaction contributed up to 12% of reconstructed sea-level change (0.03 mm yr^{-1}), but did not generate artificial trends. Following decompaction and adjustment for regional land-level change, the reconstructed rate of sea-level rise since ~AD 1850 was 1.71 mm yr^{-1}. Our study demonstrates that routine 'decompaction' of salt marsh sediments can be undertaken if suitable modern analogues are available. We therefore recommend the development and application of regional datasets that describe the compression properties of sediments from a range of salt-marsh environments.

Study sites

Our primary study site is Tump Point, located in southwestern Pamlico Sound, North Carolina, USA (Figs. 1A–C). Pamlico Sound is a wide, shallow estuarine system that separates the mainland of North Carolina from the barrier island system of the Outer Banks. Tump Point is typical of organogenic salt marshes in this region that are comprised of extensive platforms (often several km wide) of *Juncus roemerianus* salt marsh (Figs. 1B–E) with a narrow (~5 m), seaward fringe of *Spartina alterniflora*, interspersed with occasional patches of *Distichlis spicata*, *Borrichia frutescens* and *Spartina patens* (e.g., Adams, 1963; Eleuterius, 1976; Brinson, 1991; Woerner and Hackney, 1997). The salt-marsh platform at Tump Point is not dissected or flooded/drained by tidal channels.

Levelling transects up to 4 km long show that elevation varies by less than 0.25 m over the majority of the site (Brinson, 1991). This low range in elevation results from the microtidal regime present at the site; the modern diurnal range (mean lower low water to mean higher high water) is 0.13 m (Kemp et al., 2009). The lack of spatial variability in contemporary salt-marsh geomorphology and ecology is reflected in a near-uniform stratigraphy that varied little in a transect of cores covering several hundred metres (Kemp et al., 2009; Figs. 1D, E). The modern salt marsh is underlain by a pre-Holocene sand (assumed incompressible) with a black, amorphous basal unit that transitions upward into 1.2–1.5 m of salt-marsh peat that spans the period since ~AD 1000 and contains abundant and in situ *J. roemerianus* macrofossils. The small tidal range and undisturbed accumulation of salt-marsh peat make Tump Point sensitive to small changes in sea level and ideal for reconstructing late Holocene RSL.

It is worth noting that the physiographic and ecological conditions at Tump Point differ considerably from the minerogenic marshes encountered in northwest Europe that typically have meso- to macrotidal regimes, have large elevational changes and are characterized by deposition of clastic sediment that is distributed by tidal creeks (Allen, 2000). This results in more pronounced variability in sedimentation at

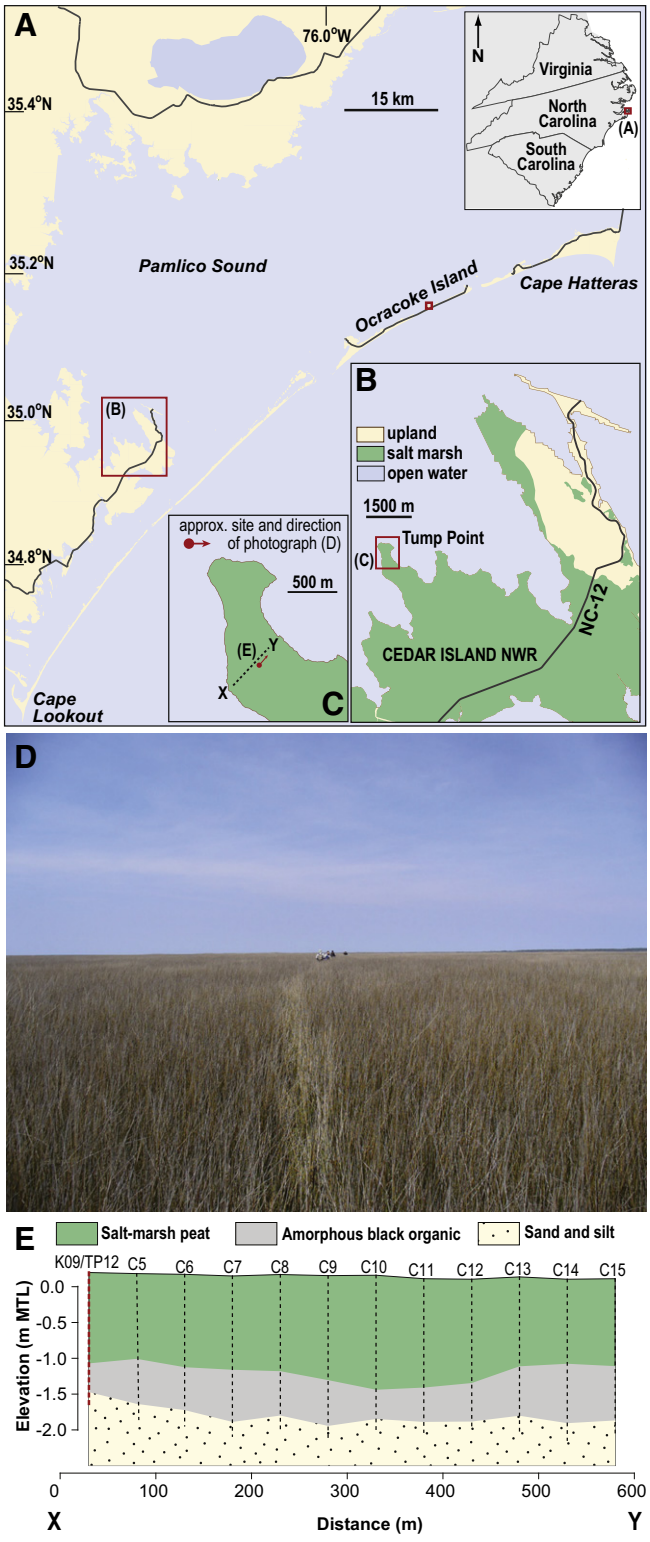

Figure 1. (A–C) Locations of study sites at Tump Point and Ocracoke Island, North Carolina, USA. (D) Photograph of the flat, extensive and ecologically homogeneous salt-marsh platform at Tump Point. Approximate location and direction of view of the photograph are displayed in (C). (E) Simplified stratigraphy underlying the Tump Point site. Adapted from Kemp et al., 2009.

https://doi.org/10.1016/j.yqres.2014.08.003 Published online by Cambridge University Press

a variety of spatial scales within a single salt marsh (e.g., Stoddart et al., 1989; French and Spencer, 1993; Allen, 2000; Plater and Appleby, 2004).

Our secondary study site is Ocracoke Island (Fig. 1A), specifically the brackish tidal flats of the northern (Pamlico Sound) coast. The Ocracoke salt marsh differs to Tump Point because it is a narrow (<500 m wide) back-barrier marsh on the Outer Banks, although the vegetation is also dominated by *J. roemerianus*. Due to the proximity of beaches and dunes, back-barrier salt marshes on the Outer Banks (including Ocracoke) typically have a higher sand and silt content than the peat that is typical of the platform marshes.

Methods

Surface samples

We obtained undisturbed sediment samples (15-cm diameter, 15-cm depth) from the modern depositional surface for laboratory geotechnical testing. To provide samples representing depositional environments analogous to those represented in the Tump Point stratigraphy, we focused primarily on the *J. roemerianus* zone ($n = 7$), but also obtained samples from patches of mixed vegetation ($n = 3$). We also collected a single sample of sand from Ocracoke Island (Fig. 1A) to provide a regionally-collected modern analogue for the sandy, amorphous basal unit in the Tump Point core. Further description of each surface sample is provided in Table 1. All core and surface samples were stored in confined, sealed and cold (~4°C) conditions prior to testing to prevent disturbance due to stress relief and moisture loss and to limit the operation of bacterial processes.

For each surface sample, we determined loss on ignition (LOI), bulk density, moisture content, specific gravity (G_s), and voids ratio (e) by Height of Solids following the methods in Head (1980). These measurements characterized the sediment and were used in compaction model equations (Brain et al., 2012). Reported LOI values for each surface sample represent the mean of three determinations to assess variability in small sample masses (approximately 2 g of dry mass following desiccation to determine moisture content; see Heiri et al., 2001) (Table 2). All other results represent one determination. We undertook one-dimensional, zero-lateral strain compression testing using fixed ring, front-loading oedometers (Head, 1988). Each loading stage lasted until dissipation of excess pore water pressure, as determined from plots of settlement against square-root time (Head, 1988). Using the oedometer compression test results for each sample, we estimated values for each of the parameters of the Brain et al. (2011, 2012) framework, which describes changes in e (a volumetric parameter) in response to changes in vertical effective stress, σ' (kPa). Four variables define the framework: e_1 is a constant defining e at 1 kPa; C_r is the recompression index, which describes changes in e with the common logarithm of σ' ($\log \sigma'$) in the reduced compressibility (overconsolidated) stress range; C_c is the compression index, which describes changes in e with $\log \sigma'$ in the normally consolidated stress range; and σ'_y is the yield stress, which defines the value of σ' at which compressibility increases, marking the transition from over- to normally consolidated behaviour. Overconsolidated ('pre-compressed') sediments have experienced an effective compressive stress greater than that exerted by the existing overburden (Head, 1988). We estimated σ'_y by determining the vertical effective stress at which best-fit recompression and compression lines intersected in $e\log \sigma'$ space (cf. Brain et al., 2012).

Core samples

We collected a core of salt-marsh sediment from Tump Point in May 2012 using a Russian corer to minimise disturbance during recovery. This replicate core (TP12) was collected immediately adjacent (<1 m horizontal distance) to the core (K09) analysed by Kemp et al. (2009, 2011). The two cores have the same thickness (1.66 m) and lithostratigraphy (Figs. 2 and 3). Use of replicate cores from one coring site in late Holocene sea-level research is an established and accepted method for sites with a clear and stable stratigraphy (Varekamp et al., 1999) such as the flat, expansive platform marshes that are common in North Carolina (e.g., Tump Point) where differences in stratigraphy are negligible. In Connecticut for example, van de Plassche et al. (1998) and van de Plassche (2000) used original and published (Varekamp et al., 1992) data to demonstrate that age–depth models developed for salt-marsh cores located up to 25 m apart can be validly transferred. Similarly, Edwards et al. (2004) presented foraminifera data from replicate cores collected 6.5 m apart; both cores displayed the same pattern, sequence, and magnitude of change in reconstructed marsh surface elevation.

Table 1
Description of modern surface samples collected in North Carolina in May 2012.

Sample ID	Description of vegetation assemblage and details of salt-marsh surface characteristics
Tump Point	
TP12/GT01	Approximately 80% coverage of substrate. Vegetation dominated by *Juncus roemerianus* (95%) with *Distichlis spicata* (<5%). Waterlogged conditions, groundwater table at marsh surface. Organic muddy surface beneath covering of dead vegetation (≤1 cm thick).
TP12/GT02	Approximately 80% coverage of substrate. Vegetation dominated by *Juncus roemerianus* (95%) with *Distichlis spicata* (<5%). Waterlogged conditions, groundwater table at marsh surface. Organic muddy surface beneath covering of dead vegetation (≤1 cm thick).
TP12/GT02/B	Approximately 80% coverage of substrate. Vegetation dominated by *Juncus roemerianus* (95%) with *Distichlis spicata* (<5%). Waterlogged conditions, groundwater table at marsh surface. Organic muddy surface beneath covering of dead vegetation (≤1 cm thick).
TP12/GT03	Approximately 80% coverage of substrate. Vegetation dominated by *Juncus roemerianus* (95%) with *Distichlis spicata* (<5%). Waterlogged conditions, groundwater table at marsh surface. Organic muddy surface beneath covering of dead vegetation (≤1 cm thick).
TP12/GT04	Approximately 80% coverage of substrate. Vegetation dominated by *Juncus roemerianus* (95%) with *Distichlis spicata* (<5%). Waterlogged conditions, groundwater table at marsh surface. Organic muddy surface beneath covering of dead vegetation (≤1 cm thick).
TP12/GT05	Approximately 80% coverage of substrate. Vegetation dominated by *Juncus roemerianus* (95%) with *Distichlis spicata* (<5%). Waterlogged conditions, groundwater table at marsh surface. Organic muddy surface beneath covering of dead vegetation (≤1 cm thick).
TP12/GT06	Approximately 90% coverage of substrate. Vegetation dominated by *Distichlis spicata* (60%) with *Borrichia frutescens* (30%) and *Spartina patens* (10%). Groundwater level approximately 5 cm beneath marsh surface. Surface covered by ≤ 2 cm thick black, muddy (possibly algal) surface layer.
TP12/GT07	Approximately 80% coverage of substrate. Vegetation dominated by *Juncus roemerianus* (95%) with *Distichlis spicata* (<5%). Waterlogged conditions, groundwater table at marsh surface. Organic muddy surface beneath covering of dead vegetation (≤1 cm thick).
TP12/GT08	Approximately 90% coverage of substrate. Vegetation dominated by *Distichlis spicata* (60%) with *Spartina patens* (15%), *Spartina alterniflora* (10%), *Borrichia frutescens* (10%) and *Salicornia virginica* (<5%). Groundwater level approximately 10 cm beneath marsh surface. Surface covered by ≤ 2 cm thick black, muddy (possibly algal) surface layer and organic, desiccated sea wrack.
TP12/GT09	Approximately 90% coverage of substrate. Vegetation dominated by *Spartina patens* (80%) with *Borrichia frutescens* (10%) and *Spartina alterniflora* (10%). Groundwater level approximately 5 cm beneath marsh surface. Organic muddy surface beneath covering of dead vegetation (≤1 cm thick).
Okracoke Island	
OCR12/GT01	Brown medium sand with occasional rootlets. Some *Spartina alterniflora* and *Spartina patens* (c. 20% coverage).

https://doi.org/10.1016/j.yqres.2014.08.003 Published online by Cambridge University Press

Table 2
Results of geotechnical tests performed on modern samples collected in North Carolina in May 2012. Loss on ignition results (mean and standard deviation, SD) are based on three determinations for each sample. Standard deviations are expressed as percentage points.

Sample ID	Loss on ignition (%)		Specific gravity, G_s	Voids ratio at 1 kPa, e_1	Recompression index, C_r	Compression index, C_c	Yield stress, σ'_y (kPa)	Saturated bulk density (g cm^{-3})
	Mean	SD						
Tump Point								
TP12/GT01	36.60	1.90	2.13	9.96	0.11	3.80	3.5	1.11
TP12/GT02	42.17	4.22	2.10	10.32	0.22	3.93	3.5	1.09
TP12/GT02/B	51.50	3.10	2.06	10.75	0.48	4.02	3.5	1.07
TP12/GT03	30.73	3.15	2.14	7.52	0.15	3.22	4.0	1.13
TP12/GT04	34.43	0.87	2.18	8.40	0.24	3.09	3.5	1.12
TP12/GT05	40.79	2.80	2.01	7.83	0.15	3.22	4.0	1.11
TP12/GT06	35.44	2.26	2.05	7.83	0.10	3.12	4.0	1.12
TP12/GT07	48.20	1.38	2.10	10.60	0.42	3.98	3.5	1.08
TP12/GT08	43.87	1.92	2.22	9.54	0.17	3.75	4.5	1.10
TP12/GT09	34.56	3.25	2.15	7.26	0.12	3.24	4.5	1.14
Okracoke Island								
OCR12/GT01	0.65	0.09	2.64	1.15	0.01	0.21	4.5	1.70

We sampled TP12 by slicing the core into 2-cm-thick contiguous samples, which is the approximate height of a typical oedometer sample (Brain et al., 2012). For each core sample, we estimated organic content by LOI and measured bulk density following the methods described by Head (1980). We use LOI as a proxy for organic content because it is quickly determined and routinely collected (Dean, 1974; Heiri et al., 2001; Brain et al., 2012). To measure LOI, we subjected oven-dried (105°C for 24 h) sediment samples to ignition temperatures of 550°C for 4 h to maximise the combustion of organic material, minimise the loss of interstitial water from clay minerals, and limit the breakdown of carbonates at higher temperatures (Head, 1980; Heiri et al., 2001; Boyle, 2004).

Modelling and validation approach

Our decompaction modelling approach takes LOI variability into consideration to ensure that minor differences in LOI (and hence compaction behaviour) are not over-interpreted (Heiri et al., 2001). We note from Table 2 that LOI values measured in surface sediment vary even among sub-samples collected from within a few mm to cm of each other. Given the proximity of these sub-samples, we attribute such variability in LOI to inherent and unavoidable variability in high salt-marsh peat resulting from differences in root and rhizome content, for example, rather than meaningful changes in salt-marsh facies over such small distances. In space-for-time substitution it is therefore reasonable to expect that LOI could also vary to a similar degree within a single core and between immediately adjacent cores. Such differences would also be observed in other measurements of organic content, such as total organic content, given the relatively small sample size obtained using a Russian core (e.g., Kemp et al., 2012).

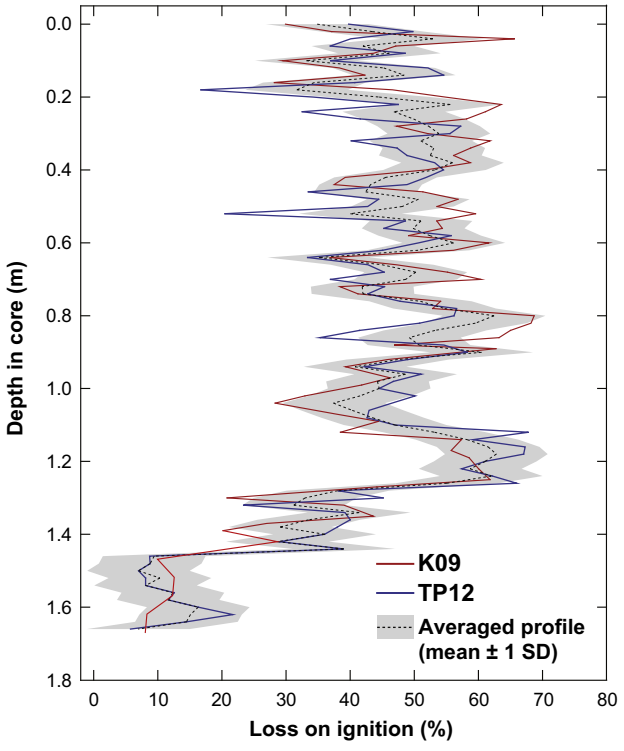

Figure 2. Measured and averaged (±1 standard deviation, SD) downcore loss on ignition in cores K09 and TP12.

The combination of LOI measurements from TP12 and K09 allows us to consider the effects on compaction of the inevitable and minor stochastic variability in downcore lithology and provides measurements of bulk density that were not collected by Kemp et al. (2009). Our modelling and validation approach for handling the K09 and replicate TP12 cores can, therefore, be summarised as follows and each step is detailed further in subsequent sections.

Our start and end point is the K09 core, for which Kemp et al. (2009, 2011) reconstructed palaeomarsh elevation using foraminifera and developed a multi-proxy age–depth model to produce a late Holocene sea-level curve for Tump Point. Only the elevation (sea-level) component of the reconstruction requires correction for the effects of sediment compaction. The reconstructed sea-level trend and chronology for K09 are not transferred to TP12 in our study. To consider the natural variability in downcore LOI, we firstly calculated the mean (with associated uncertainty) LOI of cores K09 and TP12 at each depth to create a combined ('averaged') LOI profile (Fig. 2). Since the Brain et al. (2011, 2012) compression modelling framework only considers changes in effective stress, estimates of PDL depend only on downcore lithostratigraphy (LOI) and are independent of sediment age. Therefore, the role of the TP12 core is to allow generation of the averaged LOI profile and increase the probability that the 'true' compaction behaviour of K09 is adequately captured using our stochastic (Monte Carlo) decompaction modelling approach.

Secondly, we used empirical relationships between compression properties and LOI, plus stratigraphic data, to calibrate the decompaction model and to subsequently predict how the sediment compacted as overburden loading occurred. This is quantified as depth-specific estimates of PDL at 2-cm depth intervals. PDL is the height correction that is added to the in situ (measured) altitude of a sediment sample to return it to its depositional altitude.

Thirdly, we compared model predictions of downcore bulk density to those observed in core TP12 to assess the predictive capacity of the model. Finally, we corrected the K09 sea-level reconstruction for

https://doi.org/10.1016/j.yqres.2014.08.003 Published online by Cambridge University Press

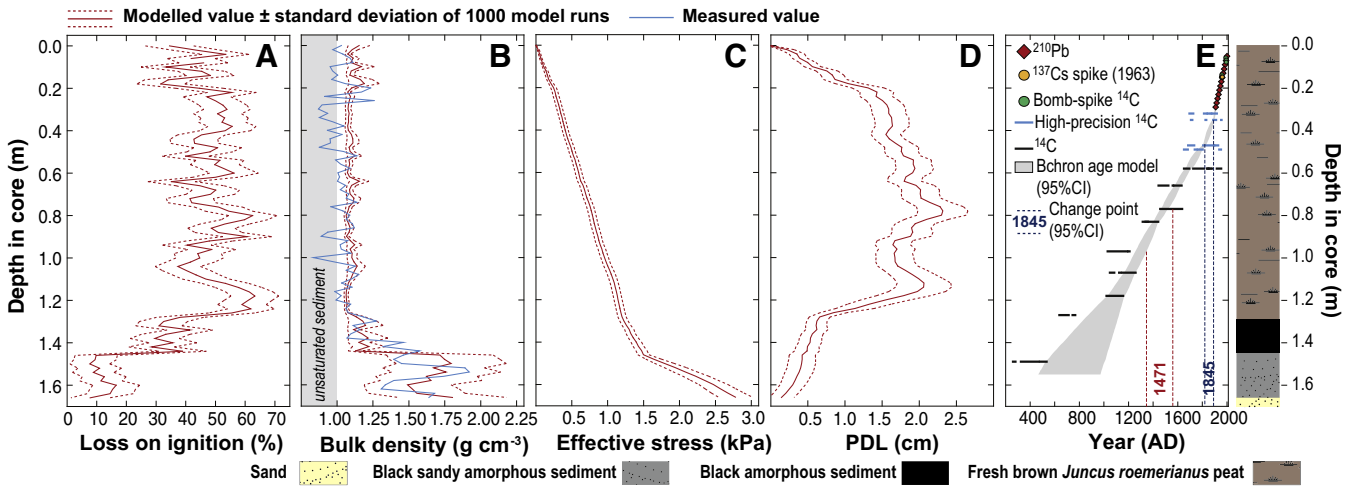

Figure 3. Geotechnical and physical properties and stratigraphy of the Tump Point core. (A) Averaged downcore organic content, expressed as % loss on ignition. (B) Measured and modelled bulk density. (C) Modelled effective stress. (D) Model estimates of post-depositional lowering (PDL) for 2-cm-thick samples. (E) Age–depth model for the K09 Tump Point core, modified from Kemp et al. (2011) and developed using Bchron (Haslett and Parnell, 2008; Parnell et al., 2008).

compaction effects using the modelled PDL outputs. This involves adding depth-specific values of PDL obtained using the averaged LOI profile to corresponding reconstructions of relative sea level for that depth in K09, linearly interpolating between adjacent (2-cm depth interval) predictions where sea-level reconstructions were obtained from depths for which PDL predictions were not directly made.

Laboratory results

Surface samples

We present the physical and compression properties of the surface samples in Table 2. The modern calibration samples from *J. roemerianus* environments had LOI values of 30.73–51.50% (mean, $\bar{x} = 40.65\%$; standard deviation, SD = 7.41%). Samples from the mixed vegetation zones had LOI values of 34.56–43.87% ($\bar{x} = 37.96\%$; SD = 5.14%). Saturated bulk densities in modern samples ranged from 1.07 to 1.14 g cm^{-3} ($\bar{x} = 1.11$ g cm^{-3}; SD = 0.02 g cm^{-3}). Modern salt marsh samples displayed e_1 values of 7.26–10.75 ($\bar{x} = 9.00$; SD = 1.37), C_r values of 0.10–0.48 ($\bar{x} = 0.22$; SD = 0.13) and C_c values of 3.09–4.02 ($\bar{x} = 3.54$; SD = 0.39). The brown medium sand sample obtained from Ocracoke Island displayed a lower e_1 value (1.15) and lower compressibility throughout the overconsolidated ($C_r = 0.01$) and normally-consolidated ($C_c = 0.21$) stress ranges. All samples displayed compressive yield stresses between 3.5 and 4.5 kPa.

Core samples

In Figure 2, we display downcore values of LOI in cores K09 and TP12. For TP12 and K09, LOI was obtained for depths of 0.00–1.66 m. Cores K09 and TP12 display similar downcore LOI profiles and the minor differences observed are within the expected range given the variability in LOI measured in sub samples of modern (surface) sediment at Tump Point (Table 2). To consider and adequately capture the observed natural variability in down-core organic content in our decompaction modelling, we calculated the mean LOI of K09 and TP12 at each depth (averaged LOI profile in Figs. 2 and 3A). We also calculated the standard deviation of the measured LOI values at each depth (2-cm-thick layers) in K09 and TP12 and subsequently calculated the mean of these standard deviations (8 percentage points) throughout the core. This serves as a quantitative description of the stochastic, intra-stratum variability in organic content at each depth and demonstrates that the majority of LOI measurements fall within this averaged error envelope (Fig. 2).

Figure 3 displays idealised stratigraphy, the averaged LOI profile at Tump Point, and the downcore bulk density profile of core TP12. LOI in the averaged profile ranged from 6.95% at the transition to underlying sand (1.66 m) to 62.78% in the *J. roemerianus* peat (1.18 m; Figs. 2 and 3A). Within the *J. roemerianus* peat and black amorphous stratum, mean LOI was 47.02% (SD = 8.67%). Greater LOI values occurred near the base of the *J. roemerianus* stratum (1.12–1.27 m). The black sandy amorphous layer (1.45–1.66 m) was characterized by LOI values (6.95–16.32%) lower than those observed in our surface samples. More than half (57%) of the downcore LOI measurements fell within the range measured in modern samples.

Bulk density measured downcore in core TP12 reflects the visual stratigraphy (Fig. 3B). Within the *J. roemerianus* peat, mean bulk density was 1.02 g cm^{-3}. Measured bulk density values < 1 g cm^{-3} reflect high sediment permeability; once removed from the ground, these core sediments partially drained and became unsaturated (Hobbs, 1986). Bulk density increases in the underlying black amorphous material ($\bar{x} =$ 1.25 g cm^{-3}) and again within the black sand ($\bar{x} = 1.56$ g cm^{-3}).

Modelling compaction

Controls on compression behaviour

Comparison of observed trends in e_1, C_r, C_c and G_s with LOI measured in the modern Tump Point sediments with those presented for a multi-site compilation of United Kingdom (UK) salt-marsh sediments (LOI range = 1.32–40.37%) by Brain et al. (2012) demonstrates similarity at comparable LOI values (Fig. 4). The Tump Point data extend the trends observed in the UK data to LOI values > 40.37%. This inter-site agreement supports the assertion by Brain et al. (2011, 2012) that organic content exerts a common, first-order control on near-surface structure and compressibility of salt-marsh sediments despite inter-site differences in geomorphic, hydrographic, climate, and ecological conditions. The observed relationships result from the creation of highly porous sediment structures by vascular plants (DeLaune et al., 1994). Low-density sediments are more prone to compression than those with greater minerogenic content (Brain et al., 2011).

Variations of σ'_y in salt-marsh sediments are caused by differences in effective stress history at the depositional surface. Such differences result from falls in groundwater level and/or subaerial desiccation (Brain et al., 2011, 2012). At Tump Point, measured σ'_y ranged between ~3.5 and 4.5 kPa. This limited variability in σ'_y likely reflects the low tidal and elevation range. These local conditions maintain a near-surface groundwater table and waterlogged conditions and prevent large

https://doi.org/10.1016/j.yqres.2014.08.003 Published online by Cambridge University Press

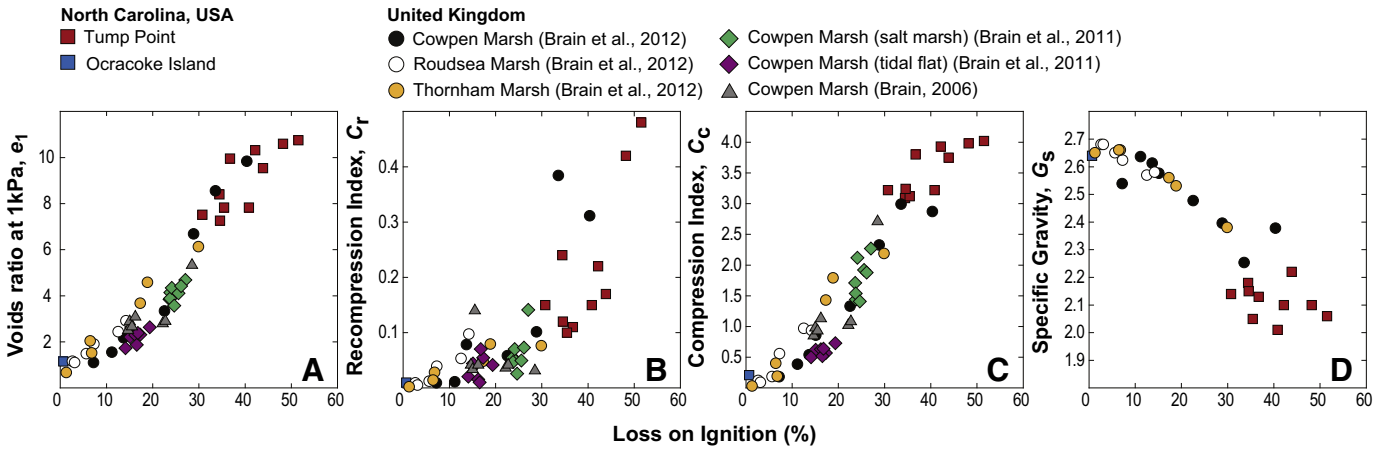

Figure 4. Observed relationships between geotechnical (A–C) and physical properties (D) of salt-marsh sediments used for model calibration. United Kingdom data are from Brain (2006), Brain et al. (2011) and Brain et al. (2012).

variations in surface topography from forming, such that differences in subaerial exposure, desiccation and, hence, σ'_y are negligible at Tump Point.

Model calibration

We define statistically significant ($p < 0.0001$) predictive relationships between LOI and e_1, C_r, C_c and G_s by combining the Tump Point and UK datasets. This permits downcore estimation of these properties and calibration of the Brain et al. (2011, 2012) compaction model using the measured LOI values displayed in Figure 3A. Fitted equations used to predict geotechnical and physical properties from LOI values are displayed with key regression statistics in Table 3. The combined dataset provides modern analogues for the majority (73%) of samples in the Tump Point core (Figs. 2, 3; Table 2). Application of the relationships and equations summarised in Table 3 to the LOI values measured in the Tump Point core(s) requires extrapolation where modelled LOI > 51.50%. However, comparison of predictions of e_1, C_r, C_c and G_s at these greater LOI values with measurements from salt-marsh sediments with greater organic content (maximum LOI = 86%) by Cullen (2013) demonstrates reasonable agreement. We note, however, that some minor inter-site differences may exist and so we base our regression models on the datasets presented in Figure 4 and use minor extrapolation of observed trends.

To calibrate and run the Brain et al. (2011, 2012) compaction model, we used our averaged core profile—i.e., the calculated mean and standard deviation of LOI values measured at each depth (2-cm-thick layers) in cores K09 and TP12. The initial model input, therefore, comprises the mean LOI value of the two cores with a normally distributed error term, of which the standard deviation is 8 percentage points. In each model run, a LOI value was selected by the model for every 2-cm-thick core sample downcore according to this defined probability distribution. Subsequently, and again in each model run, the selected value was used to predict geotechnical and physical properties for each downcore sample using the equations presented in Table 3. We ran the model 1000 times to generate a large sample dataset; each model run represents a feasible set of physical and geotechnical properties within the core. Hence, by averaging LOI between cores and by defining an appropriate error therein, we are able to better constrain the potential variability in compaction behaviour, rather than relying on the LOI results of a single core for which a single set of downcore LOI readings may not be fully representative for the reasons noted above regarding the presence and nature of plant macrofossil content. Where appropriate, we used the standard error of the estimate as our regression model error. However, following Brain et al. (2012), where the form of the residuals deviates from a normal distribution (i.e., if the residuals failed a Shapiro–Wilk normality test) we used a uniformly distributed error term (± half the range of the modelled residuals). Regression-model error term estimations are provided in Table 4. The resulting sample of 1000 estimates of LOI and physical properties was used to estimate PDL.

Table 3
Predictive equations used to estimate key compression and physical properties using averaged downcore loss on ignition (LOI) values.

Equation	r^2_{adj}	p
$G_s = 2.7288 + (-0.0139 \times \mathrm{LOI})$	0.86	<0.0001
$e_1 = \frac{12.8408}{1+\exp\left(-\frac{\mathrm{LOI}-30.7401}{10.4283}\right)}$	0.94	<0.0001
$C_r = 0.0026 + (0.0134(\exp(0.0690 \times \mathrm{LOI}))$	0.74	<0.0001
$C_c = \frac{4.1349}{1+\exp\left(-\frac{\mathrm{LOI}-26.6509}{7.4981}\right)}$	0.94	<0.0001

Post-depositional lowering

The key output of a (de-)compaction model is depth-specific estimates of PDL. We used the repeat-iteration, stochastic (Monte Carlo; 1000 model runs) approach and assumptions detailed by Brain et al. (2012) to constrain the effects of inter- and intra-core variability and uncertainty in input values and estimates of e_1, C_r, C_c and G_s. We 'split' the sediment core into 2-cm-thick layers for modelling. Within each layer, we defined values of σ'_y between 3.5 and 4.5 kPa at all depths in the core and assigned compression properties based on the observed empirical relationships with LOI.

Starting with the uppermost layer and assuming fully saturated in situ conditions and a positive, hydrostatic pore water pressure profile (a reasonable assumption given the low tidal and elevation ranges and surface groundwater levels observed at Tump Point), we calculated bulk density and effective stress profiles by iteration (Figs. 3B, C). The estimated effective stress at the base of the core is 2.78 ± 0.24 kPa. Notably, this is less than the lowest modelled σ'_y, demonstrating that the sediments throughout the core are overconsolidated and remain in their reduced-compressibility condition at all depths. Modelled bulk density values reproduced observed inter-stratum trends in core TP12 well (Fig. 3B).

To estimate PDL in each layer, we subtracted the estimated effective stress value at the base of the overlying layer to obtain a new downcore effective stress profile, from which changes in e and, hence, thickness were calculated within each underlying layer (Brain et al., 2012).

https://doi.org/10.1016/j.yqres.2014.08.003 Published online by Cambridge University Press

Table 4
Summary of error terms for regression equations used in decompaction modelling. All predicted variables are dimensionless.

Predicted (predictor) variable	Residuals passed Shapiro–Wilk normality test?	Regression model error distribution	± error term
G_s (loss on ignition)	Yes	Normal	0.09[a]
e_1 (loss on ignition)	Yes	Normal	0.72[a]
C_r (loss on ignition)	No	Uniform	0.18
C_c (loss on ignition)	Yes	Normal	0.30[a]

[a] Error term is one standard error.

Summation of layer thickness changes in all underlying layers provides an estimate of PDL (Fig. 3D). There is no PDL at the top and base of the Tump Point core, whilst the peak value (2.3 ± 0.3 cm) occurred at 0.78 m (AD 1478 ± 30 yr) within the *J. roemerianus* stratum, which also shows variability in PDL caused by intra-stratum variations in LOI. The most sharply-defined inflections in the PDL curve occur at depths of 0.22 m and 1.12 m, corresponding to ages of AD 1935 ± 5 and 1160 ± 59 yr, respectively. Errors for the estimates of PDL (maximum = 0.004 m at 1.14 m; mean = 0.002 m, standard deviation = 0.001 m) are an order of magnitude lower than the precision of the transfer function used to reconstruct RSL in North Carolina salt marshes (0.03–0.05 m; Kemp et al., 2009). PDL errors are sufficiently small to preserve the overall precision of sea-level reconstructions.

Model validation

We assessed the predictive capacity of the Brain et al. (2011, 2012) compaction model by comparing model estimates of bulk density with those measured in the TP12 core. Linear regression of predicted and observed values showed good agreement ($r^2_{adj} = 0.65$), statistical significance ($p < 0.001$) and, hence, satisfactory model performance. Figure 5 demonstrates that values of predicted bulk density show broad parity with measured values, clustering around the 1:1 line, particularly when errors in predicted bulk density are considered (Fig. 5). We note, however, the more limited agreement between observed bulk densities < 1 g cm^{-3} and corresponding predicted values. Assuming that this inequality results from drainage and unsaturation of sediments following removal from the ground, we removed data points displaying observed bulk densities < 1 g cm^{-3} (Fig. 5B). This marginally improves agreement between observed and predicted values ($r^2_{adj} = 0.67$; $p < 0.001$) and the overall pattern of observed bulk density in TP12 is well reproduced by the model (see also Fig. 3B).

Bayesian changepoint regression modelling

Since the Kemp et al. (2009, 2011) North Carolina sea-level record is a two-site composite based also on data from Sand Point, we reanalysed the Tump Point reconstruction in isolation, prior to correcting for PDL. After a constant rate of land subsidence was subtracted from the in situ reconstruction (0.9 mm yr^{-1}; Engelhart and Horton, 2012), we used error-in-variables Bayesian changepoint regression modelling (Carlin et al., 1992; Spiegelhalter et al., 2002) to identify and quantify late Holocene sea-level trends with 95% confidence (Fig. 6). This revealed three successive linear trends, showing sea-level rise from AD 1000 until 1470 at 0.35 mm yr^{-1}. Sea level subsequently fell until AD 1845 (−0.24 mm yr^{-1}), when it began to rise at 1.78 mm yr^{-1}.

We then corrected the Kemp et al. (2009, 2011) in situ reconstruction of sea level for the effects of compaction by adding depth-specific values of PDL obtained using the averaged LOI profile to the corresponding sea-level reconstruction from core K09. After adjusting this new PDL-corrected RSL reconstruction for land subsidence, we analysed it using error-in-variables Bayesian changepoint regression modelling. This analysis also identified three successive linear trends. There are minimal differences in the timing and rate of trends between the in situ and the PDL-corrected reconstruction (Fig. 6). We examined the effect of compaction and PDL on the sea-level record for each linear trend by expressing the difference between the in situ and PDL-corrected reconstructions at estimate mid-points as a percentage of the in situ reconstruction. Sediment compaction contributes negligibly (0.002 mm yr^{-1}; 1% of in situ rates at estimate mid-points) to reconstructed rates during the first phase of sea-level rise (AD 1000–1470). The maximum relative contribution (0.03 mm yr^{-1}; 12%) of compaction occurs during the second sea-level trend (AD 1470–1845) and results from both the lower rate of sea-level change and the magnitude of PDL for samples in this age range (Figs. 3D, E). The PDL-corrected rate of rise since 1843 is 1.71 mm yr^{-1}, a difference of 0.07 mm yr^{-1} (4%) from the in situ rate.

Sensitivity analysis

The regression equations used to predict G_s (linear model), e_1 and C_c (three-parameter sigmoidal model) result in some, albeit minimal,

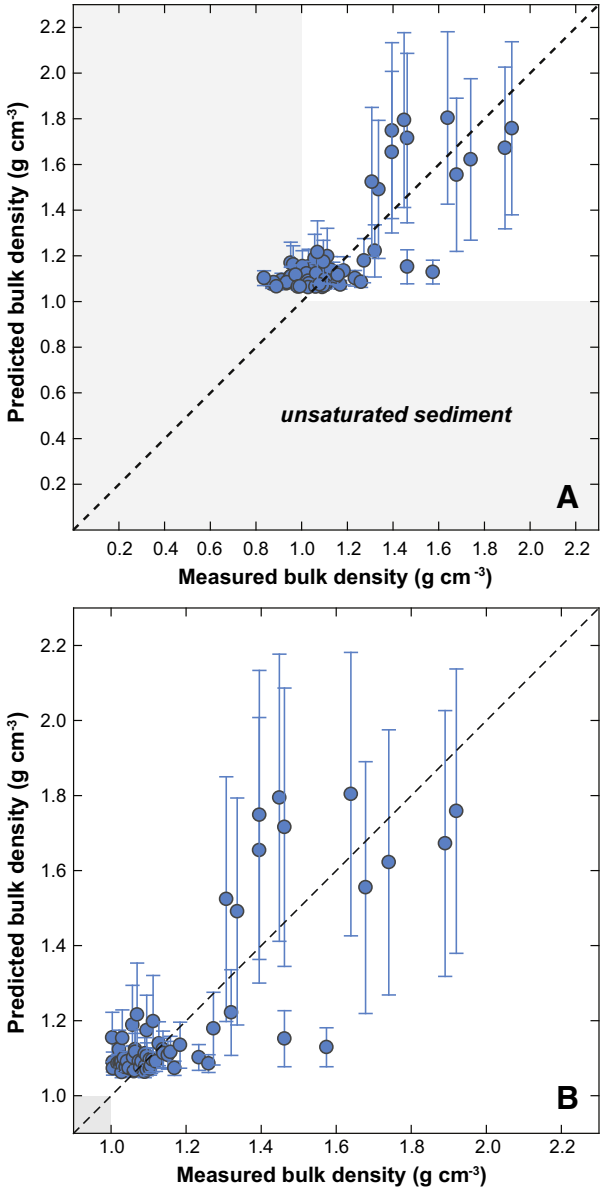

Figure 5. Plots of model-predicted against observed bulk density for the Tump Point core. (A) Full dataset. (B) Data points with observed bulk density < 1 g cm^{-3} (i.e., unsaturated sediments) removed. Error bars for values of predicted bulk density represent the standard deviation of the mean of 1000 model runs.

https://doi.org/10.1016/j.yqres.2014.08.003 Published online by Cambridge University Press

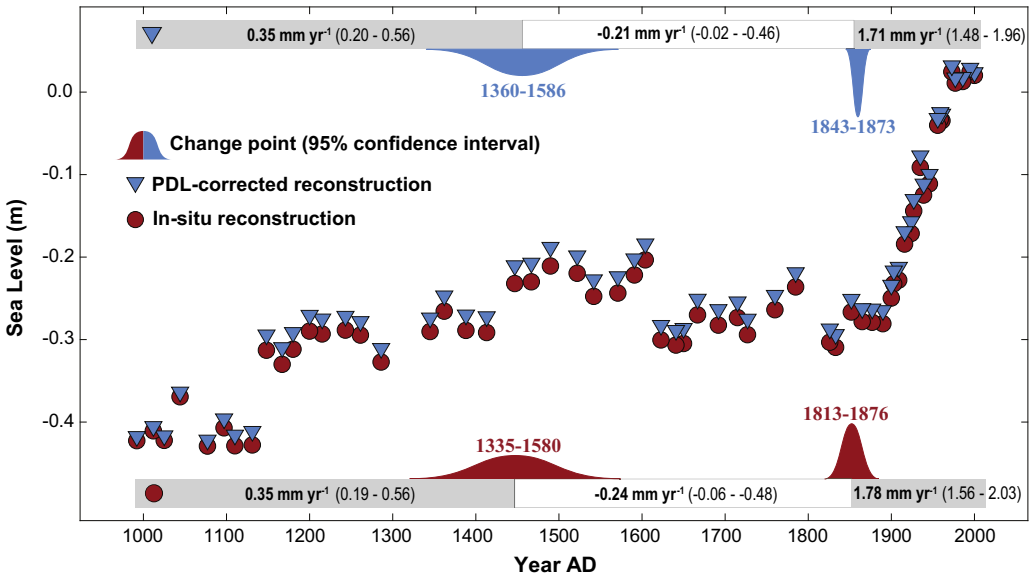

Figure 6. Reconstructed sea-level changes at Tump Point following correction for land-level change (0.9 mm yr^{-1}). An error-in-variables changepoint model identified persistent sea-level trends for the in situ (red circles) and decompacted (blue triangles) reconstructions. For clarity, reconstructions are presented as estimate mid points without vertical or temporal uncertainties (see Kemp et al., 2011).

extrapolation of values beyond those observed in the US and UK database of geotechnical and physical properties (Fig. 4; Tables 3 and 4). In addition, as we note above, predicted values of these variables in the extrapolated range broadly agree with observations made by Cullen (2013). In contrast, we fitted an exponential model to the C_r dataset. This can result in prediction of potentially unrealistic values of C_r where LOI > ca. 70% that are greater than those observed elsewhere (cf. Cullen, 2013). Whilst there are few values of LOI within the averaged core profile greater than this value (see Figs. 2 and 3A), the specified normally distributed error term for LOI input values may select LOI values greater > 70% in some model iterations. Hence, this may result in generation of C_r values that are in excess of those observed in real-world salt-marsh sediments (cf. Cullen, 2013). To assess the sensitivity of predicted post-depositional lowering (PDL) and, hence, sea-level reconstructions to the form of the C_r regression equation, we re-ran the model with a specified maximum C_r value of 1.26, equal to the maximum value observed by Cullen (2013). The mean downcore difference in PDL was minimal at 3.29% (standard deviation = 3.34%). Using the PDL outputs of this sensitivity check, we again corrected the in situ sea-level reconstruction and re-ran error-in-variables changepoint analysis (Table 5). The resultant changepoints and rates of change also demonstrate only very minor differences to the primary model run that uses the exponential regression model to predict C_r. As such, we conclude that our assumptions are fair and that our conclusions hold.

Discussion

Sediment compaction does not provide a causal mechanism for, or dramatically exaggerate, reconstructed sea-level trends at Tump Point despite the coincidence (at 0.78 m) of the ~AD 1470 changepoint with the peak PDL value. By using an empirically-informed, locally-calibrated and validated geotechnical model, we further demonstrate the value and robustness of the salt-marsh method for reconstructing late Holocene sea level.

Absolute PDL values estimated for the Tump Point core are unlikely to cause significant misinterpretation of climate- and cryosphere-related forcing of sea-level. However, low magnitudes of PDL may be important when trying to identify sea-level fingerprints of ice-sheet melt (Mitrovica et al., 2001) through comparison with other salt-marsh reconstructions (Engelhart et al., 2009) and/or tide-gauge records (Douglas, 1991). In addition, such minor effects may be important if semi-empirical sea-level models that are calibrated using salt-marsh reconstructions amplify the ostensibly subtle effects of compaction on sea level non-linearly (cf. Kemp et al., 2011; Bittermann et al., 2013).

The decompacted rate of sea-level rise since ~AD 1850 (1.71 mm yr^{-1}) approximates rates observed over similar timeframes in regional (Zervas, 2004) and globally-averaged (Douglas, 1991; Church and White, 2006; Jevrejeva et al., 2008; Woodworth et al., 2009; Church and White, 2011) tide-gauge records. This agreement is of interest because the North Carolina late Holocene sea-level record has been presented as a pseudo-global reconstruction and, hence, was used to calibrate semi-empirical numerical models to predict future global sea-level change in response to projected temperature rise (Kemp et al., 2011).

In our Tump Point study, the contribution of compaction to reconstructed sea level is small in absolute and relative terms. In contrast, sites with deeper stratigraphies and pronounced and abrupt 'transgressive' changes in downcore lithology are prone to larger compaction-induced distortions to the sea-level record. Brain et al. (2012) used a geotechnical modelling approach to demonstrate that thick (2–3 m) sedimentary successions displaying a marked transgressive contact manifest as a notable reduction in organic content that is coincident with the timing of the increase in rate of sea-level rise are most prone to this effect. Brain et al. (2012) showed that sediment compaction in such stratigraphic sequences can contribute up to 0.4 mm yr^{-1} to rates of sea-level rise reconstructed from salt-marsh sediments during the 19th and 20th centuries. Over longer (millennial) time scales, the effects of transgressive contacts in deeper sedimentary successions are profoundly demonstrated in stratigraphic studies. For example, in the Mississippi Delta, USA, Törnqvist et al. (2008) observed >2 m variation

Table 5
Results of error-in-variables changepoint analysis undertaken on PDL- and GIA-corrected sea-level data. PDL was estimated in this case using a revised ('bounded') regression model to predict C_r to address sensitivity of results to extrapolation of values beyond the observed range.

Parameter	Mean	95% confidence intervals
Changepoint 1	1490	1379–1572
Changepoint 2	1844	1812–1873
Rate 1 (mm yr^{-1})	0.350	0.202–0.543
Rate 2 (mm yr^{-1})	−0.199	−0.421 − 0.017
Rate 3 (mm yr^{-1})	1.719	1.495–1.984

https://doi.org/10.1016/j.yqres.2014.08.003 Published online by Cambridge University Press

in elevation of an isochronous peat that was overlain with clastic material of variable thickness. Törnqvist et al. (2008) estimated millennial-time scale PDL rates of 5 mm yr^{-1} and suggested that such rates over decadal and centennial time scales may be as great as 10 mm yr^{-1}. Indeed, Long et al. (2006) documented the variable elevation of a peat-clay transgressive contact at Romney Marsh, southeast England. They suggested that an originally largely planar peat surface was locally lowered by a minimum of 4.2 m over centennial time scales and equating to a 50% reduction in peat thickness. Horton and Shennan (2009) used a sea-level database for eastern England to compare the altitudes of isochronous basal and intercalated sea-level index points. They concluded that compaction can cause PDL of up to 6 m in extreme cases. They calculated average PDL rates of 0.1–0.4 mm yr^{-1}, reaching 0.6 ± 0.3 mm yr^{-1} in larger estuarine systems that display deeper stratigraphies.

Evidently, deep, 'transgressive' sequences should be avoided in late Holocene sea-level reconstructions, and indeed this has been the case in such recent studies (Gehrels et al., 2005, 2006, 2008, Kemp et al., 2009, 2011; Gehrels et al., 2012). Nevertheless, PDL should be routinely estimated in such situations using calibrated and validated geotechnical models. This is particularly important where background rates of sea-level rise are low and are reconstructed from sediments that are stratigraphically located towards the mid-point of the sediment column, where the greatest potential exists for PDL, distortion of sea-level records and, hence, misinterpretation of compaction effects as 'real' variations in historic sea-level (Paul and Barras, 1998; van Asselen et al., 2009; Brain et al., 2012).

Our study demonstrates that use of geotechnical models to correct sea-level records for compaction-induced PDL is possible, and it is increasingly feasible that routine 'decompaction' can be undertaken. However, we have demonstrated that model calibration may require the use of modern analogues from areas not found in the local contemporary environment, despite the fact that the modern samples collected at Tump Point provide a 'training set' of modern samples from the type of extensive *J. roemerianus* salt marshes that are typical of the southeastern United States. The issue regarding the degree to which modern analogues for sediments encountered in the fossil core are found locally in the contemporary depositional environments is familiar in many fields of Quaternary palaeoenvironmental reconstruction, particularly in sea-level research. Horton and Edwards (2006), for example, detail how use of larger, regional 'training sets' of contemporary microfossil data can improve the range of modern analogues available for use in calibration of microfossil datasets for palaeo-water depths. Whereas organic content (here quantified using LOI) appears to have an inter-site control on initial sediment density (quantified by e_1) and compressibility (C_r and C_r), this has not yet been universally proven for sites not considered in our study. Furthermore, values of σ'_y respond to local, near-surface processes that cause overconsolidation, requiring local empirical calibration, and potentially refinement, of the Brain et al. (2011, 2012) compression framework.

A critical next step in using empirically-constrained geotechnical models to widely decompact cores of salt-marsh sediment is, therefore, the development of appropriate regional training sets that provide botanical and sedimentary analogues for core samples. As reconstructions of late Holocene RSL change are developed from salt-marsh sediments that formed in other, physiographically distinct regions, it will be necessary to develop new modern datasets to determine how e_1, C_r, C_r and σ'_y vary throughout the intertidal zone and subsequently to estimate the contribution of PDL to reconstructed RSL rise. Furthermore, it is possible that estimating PDL for a single core may require modern analogues from multiple sites or regions. Maintaining the example of the United States, salt marshes exist under a wide range of physiographic conditions along the Atlantic Coast. In the mid-Atlantic (e.g., New Jersey), salt-marshes are typically dominated by C_4 plants such as *S. patens* (Tiner, 1985; Kemp et al., 2012), making them ecologically distinct from the *J. roemerianus* (a C_3 species) dominated systems of the southeastern USA (Eleuterius, 1976; Chmura and Aharon, 1995) that experience a warmer climate and closer proximity to the Gulf Stream. They are also different in comparison to New England salt marshes that have a cooler prevailing climate, different coastal geomorphology and Quaternary geological history, but are dominated by many of the same (C_3) plant species (Redfield, 1972). In regions south of North Carolina (such as northern Florida), tidal marshes may also be dominated by *Cladium jamaicense* and experience sub-tropical climates (Stuckey and Gould, 2000). Globally, at latitudes between 25° and 40° North or South, depending on regional conditions, salt marshes are replaced by mangroves as the dominant intertidal ecosystem in low-energy coastal settings (Morrisey et al., 2010). Along the USA Atlantic coast the division between salt marsh and mangrove ecosystems occurs near to Cape Canaveral (~28°N). Reconstructions of late Holocene RSL are possible from sediment that was deposited in this wide variety of biological and physical settings (Bird et al., 2004; Woodroffe, 2009). Future work must focus on use collection and testing of modern samples from an equally diverse range of contemporary salt-marsh and mangrove environments in terms of eco-sedimentary, hydrographic, climatic and geomorphic conditions in order to expand the database of modern analogues available.

Collection of appropriate core samples for assessment of PDL should become a routine part of future work aiming to reconstruct sea level from salt-marsh sediments. We advocate undertaking decompaction analysis and modelling on the same cores that are analysed for sea-level indicators and in age determination. In the event that decompaction work is undertaken 'retrospectively' (i.e. after the initial sea-level reconstruction has been completed), as we have done here, we stress that robust checks between core samples must be undertaken to demonstrate replicability. Whereas we have focussed on organic content (loss on ignition), similar rapid and robust methods should be used in more minerogenic marshes (see Rahman and Plater, 2014, for example). Indeed, cross-core comparisons should involve a suitable range of litho-, bio- and chrono-stratigraphic methods sufficient to justify and demonstrate clear comparability between cores.

Conclusions

The aim of this paper was to estimate the degree to which reconstructed sea-level trends in North Carolina are an artefact of sediment compaction. Our key findings and conclusions are as follows:

1. We undertook geotechnical tests on contemporary sediments obtained from Tump Point and Ocracoke Island, North Carolina. These sediments are analogous to those encountered within the Tump Point core used to reconstruct sea level. Comparison of the results of these tests with a database of compression properties from UK salt marshes revealed strong similarity in behaviour, supporting previous work suggesting that organic content has an inter-site control on compressibility and initial density. This permitted the datasets to be combined to increase the range of modern analogues available for model calibration. We defined statistically-significant relationships between organic content, initial voids ratio and compression indices, permitting estimation of compression properties for sediments encountered within the Tump Point core without having to undertake detailed geotechnical testing on fossil material. We observed limited variability in near-surface stress history (yield stress), allowing full and justifiable calibration of the compaction model based on local conditions.
2. The geotechnical model reproduced patterns of bulk density observed within the Tump Point sediment core well. Observed and predicted values of bulk density at each depth in the core show good agreement and statistical significance ($r^2_{adj} = 0.67$; $p < 0.001$). This suggests that the model adequately captures the compaction processes that have historically affected the core, validating the model and the range and choice of modern analogues used in calibration.

https://doi.org/10.1016/j.yqres.2014.08.003 Published online by Cambridge University Press

3. The model produced depth-specific estimates of post-depositional lowering (PDL), which is the height correction that must be added to the in situ altitude of a sediment sample to return it to its depositional altitude. After correcting the Tump Point sea-level reconstruction for PDL, we compared the timing and rates of persistent trends in sea level in the in situ and 'decompacted' datasets. We identified three trends in each record and demonstrated that the maximum absolute contribution of compaction to reconstructed sea level is 0.07 mm yr^{-1}. This occurred during the most recent phase of rise that began ~AD 1850. The maximum relative compaction contribution (12% of reconstructed rise) occurred between 1470 and 1845. We consider these effects to be insufficient to cause significant misinterpretation of historic sea-level changes and associated forcing mechanisms.
4. By correcting a 'high resolution', late Holocene sea-level record for the effects of sediment compaction, we have shown that compaction can no longer be ignored or dismissed as an insurmountable limitation to salt-marsh reconstructions of sea level. To this end, we advocate the development and application of regional datasets that describe the compression properties of salt-marsh sediments from a wider variety of physiographic settings that display distinct botanical characteristics. For new reconstructions, analysis and modelling must be undertaken on the same cores used to reconstruct sea level. If decompaction is to be undertaken for a previously-developed reconstruction, sufficient care must be taken to demonstrate replicability of core samples.

Acknowledgments

This work was supported by the National Science Foundation (EAR 1402017) and National Oceanic and Atmospheric Administration (NA11OAR4310101). We thank Don Barber, Reide Corbett, John Woods, Ane García-Artola, Hanna Thornberg, and Ray Tichenor for their help in the field; and Neil Tunstall, Alison George and Chris Longley for laboratory support. We are grateful to the US Fish and Wildlife service for permitting collection of sediment samples in the Cedar Island National Wildlife Refuge (Special Use Permit 42530-12-004). This is a contribution to PALSEA2 and IGCP Project 588 "*Preparing for Coastal Change*". The manuscript benefited from the thoughtful and productive comments of Robin Edwards and an anonymous reviewer.

References

Adams, D.A., 1963. Factors influencing vascular plant zonation in North Carolina salt marshes. Ecology 44, 445–465.
Allen, J.R.L., 1999. Geological impacts on coastal wetland landscapes: some general effects of sediment autocompaction in the Holocene of northwest Europe. Holocene 9 (1), 1–12.
Allen, J.R.L., 2000. Morphodynamics of Holocene salt marshes: a review sketch from the Atlantic and Southern North Sea coasts of Europe. Quaternary Science Reviews 19 (12), 1155–1231.
Bird, M.I., Fifield, L.K., Chua, S., Goh, B., 2004. Calculating sediment compaction for radiocarbon dating of intertidal sediments. Radiocarbon 46, 421–435.
Bittermann, K., Rahmstorf, S., Perrette, M., Vermeer, M., 2013. Predictability of twentieth century sea-level rise from past data. Environmental Research Letters 8 (1), 01401.
Bloom, A.L., 1964. Peat accumulation and compaction in Connecticut coastal marsh. Journal of Sedimentary Research 34 (3), 599–603.
Boyle, J., 2004. A comparison of two methods for estimating the organic matter content of sediments. Journal of Paleolimnology 31, 125–127.
Brain, M.J., 2006. Autocompaction of mineralogenic intertidal sediments. Unpublished PhD Thesis, Durham University, UK.
Brain, M.J., Long, A.J., Petley, D.N., Horton, B.P., Allison, R.J., 2011. Compression behaviour of minerogenic low energy intertidal sediments. Sedimentary Geology 233 (1–4), 28–41.
Brain, M.J., Long, A.J., Woodroffe, S.A., Petley, D.N., Milledge, D.G., Parnell, A.C., 2012. Modelling the effects of sediment compaction on salt marsh reconstructions of recent sea-level rise. Earth and Planetary Science Letters 345–348, 180–193.
Brinson, M.M., 1991. Ecology of a Nontidal Brackish Marsh in Coastal North Carolina. U.S. Fish and Wildlife Service.
Carlin, B.P., Gelfand, A.E., Smith, A.F.M., 1992. Hierarchical Bayesian analysis of changepoint problems. Applied Statistics 41 (2), 389–405.
Chmura, G.L., Aharon, P., 1995. Stable carbon isotope signatures of sedimentary carbon in coastal wetlands as indicators of salinity regime. Journal of Coastal Research 11, 124–135.
Church, J.A., White, N.J., 2006. A 20th century acceleration in global sea-level rise. Geophysical Research Letters 33 (1), L01602.
Church, J., White, N., 2011. Sea-level rise from the late 19th to the early 21st century. Surveys in Geophysics 32 (4–5), 585–602.
Cullen, B.J. 2013. Decompacting a Late Holocene sea-level record from Loch Laxford, northwest Scotland. Unpublished MRes Thesis, Durham University, UK.
Dean Jr., W.E., 1974. Determination of carbonate and organic matter in calcareous sediments and sedimentary rocks by loss on ignition: comparison with other methods. Journal of Sedimentary Petrology 44, 242–248.
Delaune, R.D., Nyman, J.A., Patrick, J., W.H., 1994. Peat collapse, ponding and wetland loss in a rapidly submerging coastal marsh. Journal of Coastal Research 10, 1021–1030.
Donnelly, J.P., Cleary, P., Newby, P., Ettinger, R., 2004. Coupling instrumental and geological records of sea-level change: evidence from southern New England of an increase in the rate of sea-level rise in the late 19th century. Geophysical Research Letters 31 (5) (L05203-1-4).
Douglas, B.C., 1991. Global sea level rise. Journal of Geophysical Research 96 (C4), 6981–6992.
Edwards, R.J., van de Plassche, O., Gehrels, W.R., Wright, A.J., 2004. Assessing sea-level data from Connecticut, USA, using a foraminiferal transfer function for tide-level. Marine Micropaleontology 41, 239–255.
Eleuterius, L., 1976. The distribution of *Juncus roemerianus* in the salt marshes of North America. Chesapeake Science 17, 289–292.
Engelhart, S.E., Horton, B.P., 2012. Holocene sea level database for the Atlantic coast of the United States. Quaternary Science Reviews 54, 12–25.
Engelhart, S.E., Horton, B.P., Douglas, B.C., Peltier, W.R., Törnqvist, T.E., 2009. Spatial variability of late Holocene and 20th century sea-level rise along the Atlantic coast of the United States. Geology 37, 1115–1118.
French, J.R., Spencer, T., 1993. Dynamics of sedimentation in a tide-dominated backbarrier salt marsh, Norfolk, UK. Marine Geology 110 (3–4), 315–331.
Gehrels, W.R., Woodworth, P.L., 2013. When did modern rates of sea-level rise start? Global and Planetary Change 100, 263–277.
Gehrels, W.R., Kirby, J.R., Prokoph, A., Newnham, R.M., Achterberg, E.P., Evans, H., Black, S., Scott, D.B., 2005. Onset of rapid sea-level rise in the western Atlantic Ocean. Quaternary Science Reviews 24, 2083–2100.
Gehrels, W.R., Marshall, W.A., Gehrels, M.J., Larsen, G., Kirby, J.R., Eiriksson, J., Heinemeier, J., Shimmield, T., 2006. Rapid sea-level rise in the North Atlantic Ocean since the first half of the 19th century. The Holocene 16, 948–964.
Gehrels, W.R., Hayward, B.W., Newnham, R.M., Southall, K.E., 2008. A 20th century sea-level acceleration in New Zealand. Geophysical Research Letters 35, L02717.
Gehrels, R., Horton, B.P., Kemp, A.C., Sivan, D., 2011. Two millennia of sea-level data: the key to predicting change. Eos, Transactions of the American Geophysical Union 92 (35), 289–291.
Gehrels, W.R., Callard, S.L., Moss, P.T., Marshall, W.A., Hunter, J., Milton, J.A., Garnett, M.H., 2012. High rates of sea-level rise in the Southwest Pacific from the start of the 20th century. Earth and Planetary Science Letters 315–316, 94–102.
Grinsted, A., Jevrejeva, S., Moore, J.C., 2011. Comment on the subsidence adjustment applied to the Kemp et al. proxy of North Carolina relative sea level. Proceedings of the National Academy of Sciences 108 (40), E781–E782.
Haslett, J., Parnell, A.C., 2008. A simple monotone process with application to radiocarbon-dated depth chronologies. Journal of the Royal Statistical Society: Series C: Applied Statistics 57 (4), 399–418.
Head, K.H., 1980. Manual of Soil Laboratory Testing: Soil Classification and Compaction Tests. Pentech Press, London/Plymouth, (416 pp.).
Head, K.H., 1988. Manual of Soil Laboratory Testing: Permeability, Shear Strength and Compressibility Tests. Pentech Press, London/Plymouth, (440 pp.).
Heiri, O., Lotter, A.F., Lemcke, G., 2001. Loss on ignition as a method for estimating organic and carbonate content in sediments: reproducibility and comparability of results. Journal of Paleolimnology 25, 101–110.
Hobbs, N.B., 1986. Mire morphology and the properties and behaviour of some British and foreign peats. Quarterly Journal of Engineering Geology, London 19, 7–80.
Horton, B.P., Edwards, R.J., 2006. Quantifying Holocene sea-level change using intertidal foraminifera: lessons from the British Isles. Journal of Foraminiferal Research, Special Publication 40.
Horton, B.P., Shennan, I., 2009. Compaction of Holocene strata and the implications for relative sea level change on the east coast of England. Geology 37 (12), 1083–1086.
Horton, B.P., Engelhart, S.E., Hill, D.F., Kemp, A.C., Nikitina, D., Miller, K.G., Peltier, W.R., 2013. Influence of tidal-range change and sediment compaction on Holocene relative sea-level change in New Jersey, USA. Journal of Quaternary Science 28, 403–411.
Jelgersma, S., 1961. Holocene Sea Level Changes in the Netherlands. Maastricht, Van Aelst, (101 pp.).
Jevrejeva, S., Moore, J.C., Grinsted, A., Woodworth, P.L., 2008. Recent global sea level acceleration started over 200 years ago? Geophysical Research Letters 35 (8), L08715.
Kemp, A.C., Horton, B.P., Culver, S.J., Corbett, D.R., van de Plassche, O., Gehrels, W.R., Douglas, B.C., Parnell, A.C., 2009. Timing and magnitude of recent accelerated sea-level rise (North Carolina, United States). Geology 37 (11), 1035–1038.
Kemp, A.C., Horton, B., Donnelly, J.P., Mann, M.E., Vermeer, M., Rahmstorf, S., 2011. Climate related sea-level variations over the past two millennia. Proceedings of the National Academy of Sciences 108 (27), 11017–11022.
Kemp, A.C., Vane, C.H., Horton, B.P., Engelhart, S.E., Nikitina, D., 2012. Application of stable carbon isotopes for reconstructing salt-marsh floral zones and relative sea level, New Jersey, USA. Journal of Quaternary Science 27, 404–414.
Long, A.J., Waller, M.P., Stupples, P., 2006. Driving mechanisms of coastal change: peat compaction and the destruction of late Holocene coastal wetlands. Marine Geology 225, 63–84.
Mitrovica, J.X., Tamisiea, M.E., Davis, J.L., Milne, G.A., 2001. Recent mass balance of polar ice sheets inferred from patterns of global sea-level change. Nature 409, 1026–1029.

Morris, J.T., Sundareshwar, P.V., Nietch, C.T., Kjerfve, B., Cahoon, D.R., 2002. Response of coastal wetlands to rising sea level. Ecology 83 (10), 2869–2877.
Morrisey, D.J., Swales, A., Dittmann, S., Morrison, M.A., Lovelock, C.E., Beard, C.M., 2010. The ecology and management of temperate mangroves. Oceanography and Marine Biology: An Annual Review 48, 43–160.
Parnell, A.C., Haslett, J., Allen, J.R.M., Buck, C.E., Huntley, B., 2008. A flexible approach to assessing synchroneity of past events using Bayesian reconstructions of sedimentation history. Quaternary Science Reviews 27, 1872–1885.
Paul, M.A., Barras, B.F., 1998. A geotechnical correction for post-depositional sediment compression: examples from the Forth valley, Scotland. Journal of Quaternary Science 13 (2), 171–176.
Pizzuto, J.E., Schwendt, A.E., 1997. Mathematical modeling of autocompaction of a Holocene transgressive valley-fill deposit, Wolfe Glade, Delaware. Geology 25 (1), 57–60.
Plater, A.J., Appleby, P.G., 2004. Tidal sedimentation in the Tees estuary during the 20th century: radionuclide and magnetic evidence of pollution and sedimentary response. Estuarine, Coastal and Shelf Science 60, 179–192.
Rahman, R., Plater, A.J., 2014. Particle-size evidence of estuary evolution: a rapid and diagnostic tool for determining the nature of recent saltmarsh accretion. Geomorphology 213, 139–152.
Redfield, A.C., 1972. Development of a New England salt marsh. Ecological Monographs 42, 201–237.
Spiegelhalter, D.J., Best, N.G., Carlin, B.P., Van Der Linde, A., 2002. Bayesian measures of model complexity and fit. Journal of the Royal Statistical Society, Series B (Statistical Methodology) 64, 583–639.
Stoddart, D.R., Reed, D.J., French, J.R., 1989. Understanding salt-marsh accretion, Scolt Head Island, Norfolk, England. Estuaries 12 (4), 228–236.
Stuckey, I.H., Gould, L.L., 2000. Coastal Plants from Cape Cod to Cape Canaveral. University of North Carolina Press, Chapel Hill.
Tiner, R.W., 1985. Wetlands of New Jersey. National Wetlands Inventory. U.S. Fish and Wildlife Service, Newton Corner, MA.
Törnqvist, T.E., Wallace, D.J., Storms, J.E.A., Wallinga, J., Van Dam, R.L., Blaauw, M., Derksen, M.S., Klerks, C.J.W., Meijneken, C., Snijders, E.M.A., 2008. Mississippi Delta subsidence primarily caused by compaction of Holocene strata. Nature Geoscience 1, 173–176.
van Asselen, S., Stouthamer, E., van Asch, Th.W.J., 2009. Effects of peat compaction on delta evolution: a review on processes, responses, measuring and modelling. Earth Science Reviews 92, 35–51.
van de Plassche, O., 2000. North Atlantic climate–ocean variations and sea level in Long Island Sound, Connecticut, since 500 cal yr A.D. Quaternary Research 53, 89–97.
van de Plassche, O., van der Borg, K., de Jong, A.F.M., 1998. Sea level–climate correlation during the past 1400 yr. Geology 26, 319–322.
Varekamp, J.C., Thomas, E., van de Plassche, O., 1992. Relative sea-level rise and climate change over the last 1500 years (Clinton, CT, USA). Terra Nova 4, 29–304.
Varekamp, J.C., Thomas, E., Thompson, W.G., van de Plassche, O., van der Borg, K., de Jong, A.F.M., 1999. Sea level–climate correlation during the past 1400 yr: comment and reply. Geology 27, 189–190.
Woerner, L., Hackney, C., 1997. Distribution of *Juncus roemerianus* in North Carolina tidal marshes: the importance of physical and biotic variables. Wetlands 17, 284–291.
Woodroffe, S.A., 2009. Testing models of mid to late Holocene sea-level change, North Queensland, Australia. Quaternary Science Reviews 28, 2474–2488.
Woodworth, P.L., White, N.J., Jevrejeva, S., Holgate, S.J., Church, J.A., Gehrels, W.R., 2009. Evidence for the accelerations of sea level on multi-decade and century timescales. International Journal of Climatology 29 (6), 777–789.
Zervas, C., 2004. North Carolina Bathymetry/Topography Sea Level Rise Project: Determination of Sea Level Trends. National Oceanic and Atmospheric Administration.

https://doi.org/10.1016/j.yqres.2014.08.003 Published online by Cambridge University Press